



## Technical Note

## Rapid oxidation and immobilization of arsenic by contact glow discharge plasma in acidic solution

Bo Jiang<sup>a</sup>, Ping Hu<sup>a</sup>, Xing Zheng<sup>b</sup>, Jingtang Zheng<sup>a,\*</sup>, Minghui Tan<sup>a</sup>, Mingbo Wu<sup>a,\*</sup>, Qinzhong Xue<sup>a</sup><sup>a</sup> State Key Laboratory of Heavy Oil Processing, China University of Petroleum, Qingdao 266580, Shandong, PR China<sup>b</sup> Bei Jing Sinen En-Tech Co., Ltd, Beijing 100080, China

## HIGHLIGHTS

- Preferable oxidation of As(III) was achieved in glow plasma system.
- Adding Fe(II) led to enhanced As(III) oxidation and immobilization of arsenic.
- The precipitation was amorphous ferric arsenate-bearing ferric oxyhydroxides.
- The presence of organics retarded the immobilization of arsenic.

## ARTICLE INFO

## Article history:

Received 6 July 2014

Received in revised form 2 December 2014

Accepted 20 December 2014

Available online 16 January 2015

Handling Editor: Min Jang

## Keywords:

Glow discharge plasma

As(III) oxidation

Fenton

Ferric arsenate

Immobilization

## ABSTRACT

Arsenic is a priority pollutant in aquatic ecosystem and therefore the remediation of arsenic-bearing wastewater is an important environmental issue. This study unprecedentedly reported simultaneous oxidation of As(III) and immobilization of arsenic can be achieved using contact glow discharge process (CGDP). CGDP with thinner anodic wire and higher energy input were beneficial for higher As(V) production efficiency. Adding Fe(II) in CGDP system significantly enhanced the oxidation rate of As(III) due to the generations of additional  $\cdot\text{OH}$  and Fe(IV) species, accompanied with which arsenic can be simultaneously immobilized in one process. Arsenic immobilization can be favorably obtained at solution pH in the range of 4.0–6.0 and Fe(II) concentration from 250 to 1000  $\mu\text{M}$ . The presence of organics (i.e., oxalic acid, ethanol and phenol) retarded the arsenic immobilization by scavenging  $\cdot\text{OH}$  or complexing Fe(III) in aqueous solution. On the basis of these results, a mechanism was proposed that the formed ionic As(V) rapidly coprecipitated with Fe(III) ions or was adsorbed on the ferric oxyhydroxides with the formation of amorphous ferric arsenate-bearing ferric oxyhydroxides. This CGDP-Fenton system was of great interest for engineered systems concerned with the remediation of arsenic containing wastewater.

© 2014 Elsevier Ltd. All rights reserved.

## 1. Introduction

Arsenic, existing mainly as As(III) and As(V), is a toxic metalloid introduced into terrestrial and aquatic environments through natural sources and anthropogenic activities (Mohan and Pittman, 2007). In these arsenic-contaminated waters, the concentration of arsenic varies from micromolar (up to 70  $\mu\text{M}$  in natural waters) to millimolar levels (Gräfe et al., 2004). Till now, to remedy arsenic containing wastewaters, a great deal of effort has been made on the widely used methods, such as coprecipitation, adsorption to different solids, ion exchange and membrane processes (Bissen and Frimmel, 2003). However, compared with As(V), As(III) is more toxic and mobile in aquatic ecosystem resulting in inferior

immobilization efficiency using above methods (Jiang et al., 2014a). Thus, pre-oxidation of As(III) to As(V) is considered highly desirable and beneficial for arsenic immobilization.

Up to now, a variety of advanced oxidation processes (AOPs) using ozone (Khuntia et al., 2014),  $\text{H}_2\text{O}_2/\text{UVC}$  ( $\lambda = 253.7 \text{ nm}$ ) (Lescano et al., 2011), photo catalyst (Choi et al., 2010), electro-oxidation system (Zhao et al., 2010) and sonochemical method (Neppolian et al., 2010) have been applied for As(III) oxidation. However, most of the above established technologies do not only lead to a hazard for secondary contamination with the use of chemical reagents or nano-catalysts, but need subsequent processes for the final removal of arsenic from wastewater. Thus, it is required to find more effective and environmental benign AOPs for simultaneous oxidation and immobilization detoxification of arsenic.

Electrical discharge plasma processes become outstanding for wastewater treatment owing to reagent free and environmental

\* Corresponding authors. Tel.: +86 86984637; fax: +86 546 8395190 (J.T. Zheng).  
E-mail addresses: [jtzheng03@163.com](mailto:jtzheng03@163.com) (J. Zheng), [wumb@upc.edu.cn](mailto:wumb@upc.edu.cn) (M. Wu).

compatibility (Zhang et al., 2008; Jiang et al., 2014b). Contact glow discharge process (CGDP), as one of electrical discharge plasma processes is an unconventional electrolysis process with generating  $\cdot\text{OH}$ , which has a higher oxidation potential up to  $2.8 V_{\text{NHE}}$  ( $E^0(\cdot\text{OH}/\text{H}_2\text{O})$ ) (Chen et al., 2013). Thus it has been extensively applied for organic contaminants abatement such as pesticides, dyestuffs, pharmaceuticals and phenolic compounds (Jiang et al., 2014b). However, to the best of our knowledge, the application of CGDP for aqueous hypertoxic inorganic arsenic detoxication has not been reported.

This study unprecedentedly sought to examine the applicability of CGDP for arsenic oxidation and simultaneous immobilization of arsenic species in one process. The effects of electrical discharge and solution properties on As(III) oxidation and arsenic immobilization were investigated. Besides, the experiments of quenching active radicals and adding complexing agents were also conducted to confirm the reaction mechanism in CGDP-Fenton system.

## 2. Materials and methods

### 2.1. Materials

Sodium arsenite ( $\text{NaAsO}_2$ , 97%) was supplied by Xiya Reagent. Ammoniummolybdate tetrahydrate, ethanol, antimony potassium tartrate, oxalic acid, phenol, ferrous sulfate, coumarin,  $\text{Na}_2\text{SO}_4$ ,  $\text{H}_2\text{SO}_4$ , NaF and  $\text{H}_2\text{O}_2$  were purchased from Sinopharm Chemical Reagent Co. Ltd., China. All chemical reagents were of analytical grade and used without further purification. UltraPure water (resistivity  $18.2 \text{ M}\Omega \text{ cm}$ ) was used for all experiments. Fe(II) stock solution (50 mM) was prepared by dissolving  $\text{FeSO}_4$  in 1 mM  $\text{H}_2\text{SO}_4$  with the presence of reduced iron powder. As(III) stock solution (50 mM) were prepared by dissolving appropriate amounts of  $\text{NaAsO}_2$  in 10 mM  $\text{H}_2\text{SO}_4$ .

### 2.2. Experimental procedure

The experimental apparatus consisted of a DC high voltage power supply and a reactor, as described in Fig. S1. All working solutions were freshly prepared before use by diluting the stock solution with  $\text{Na}_2\text{SO}_4$  solution, and the pH was adjusted to the desired values with concentrated solution of NaOH (5.0 M) or  $\text{H}_2\text{SO}_4$  (5.0 M). Typically, 150 mL of solution with conductivity:  $3 \text{ mS cm}^{-1}$  was treated in the plasma reactor at 550 V/100 mA. During the reaction, the solution temperature in the reactor was controlled at  $298 \pm 5 \text{ K}$  by running tap water in the outer jacket. A magnetic stirrer was used to stir the reactor. The depth of the electrode immersed in the solution was carefully adjusted to stabilize the current and input voltage with deviation less than  $\pm 3\%$ .

At the given specific time intervals, the reaction samples were withdrawn and immediately filtrated through a  $0.45 \mu\text{m}$  membrane filter, and then the concentrations of different chemical species in the filtrate were analyzed. To determine the constituent of the precipitation in this system, the precipitation was separated from solution via vacuum filtration and then redissolved in  $\text{H}_2\text{SO}_4$  solution (pH 2.0, 100 mL) for the measurements of arsenic and iron species (Paktunc and Bruggeman, 2010). All experiments were conducted in duplicate, and the relative error was less than 3%.

### 2.3. Analysis

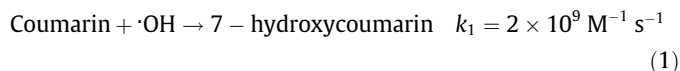
The solution conductivity and pH were measured by conductivity meter (DDS-307A) and pH meter (PHS-3C), respectively. X-ray diffraction (XRD) pattern was obtained using a Holland X'pert PRO MRD diffractometer with Cu K $\alpha$  radiation. As(V) concentration was determined using modified molybdenum-blue method (Dhar

et al., 2004), with a detection limit of  $0.03 \mu\text{M}$ . Briefly, for each 2.3 mL quenched aliquot (0.3 mL of sample + 1 mL of methanol + 1 mL of UltraPure water), 0.3 mL of the 2% HCl acidifying solution and 0.3 mL of the coloring reagent were added orderly. For total arsenic determination, 0.3 mL of the 2% HCl containing  $2 \text{ mmol L}^{-1} \text{ KIO}_3$  was used instead of 2% HCl solution. The absorbance at 880 nm was determined within 30 min using an UV-vis spectrophotometer (UV-3000, MAPADA).

$\text{H}_2\text{O}_2$  formed in the solution was determined by a spectrophotometrical method using titanium reagent (Eisenberg, 1943). 0.3 mL of the reaction mixture and 6 mL of titanium potassium oxalate (4 mM in 0.25 M sulfuric acid) were mixed together. Then the absorbance of the resulting solution was measured at 400 nm on the UV-vis spectrophotometer.

The concentration of Fe(II) ion was spectrophotometrically determined at the wavelength of 510 nm using a modified phenanthroline method (Liu et al., 2014). The premix was prepared by adding 2 mL of sodium acetate/acetic acid buffer, 2 mL of 1,10-phenanthroline solution (5.0%), and 2 mL of water (or 2 mL of ammonium fluoride solution (10%) for total iron ion concentration determination), then followed by addition of 0.5 mL of sample solution.

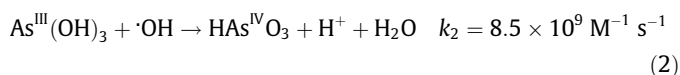
Based on Eq. (1), 1 mM coumarin was employed for probing and estimating  $\cdot\text{OH}$  in plasma system (Ishibashi et al., 2000). The fluorescence emission spectrum (excited at 332 nm) of the product 7-hydroxycoumarin (1 mL sample and 4 mL deionized water) was measured by a fluorescence spectrophotometer (F97PRO, Lengguang Tech).



## 3. Results and discussion

### 3.1. As(III) oxidation to As(V) in CGDP

In most cases, platinum is more suitable as the working anode due to its properties of corrosion resistance, high melting points and service life. However, platinum utilization greatly limits economical feasibility of CGDP for industrial applications (Jiang et al., 2014b). In present study, stainless steel wire was utilized for As(III) oxidation instead of platinum wire owing to its lower cost. Fig. 1(a) shows As(III) oxidation efficiencies using stainless steelwires with different diameters as anode and a relatively preferable As(III) oxidation rate can be obtained for 0.4 mm diameter of stainless steel wire. In this process, aqueous As(III) exists almost entirely as the nonionic  $\text{H}_3\text{AsO}_3$  at pH 4.0 (Fig. S2) and can be rapidly oxidized by OH radicals with rate constant of  $8.5 \times 10^9 \text{ M}^{-1} \text{ s}^{-1}$  (Eq. (2)) (Wang et al., 2014). One-electron oxidation of As(III) would involve the formation of the unstable As(IV) intermediate, which was further transformed to ionic As(V) (Fig. S2). Consequently, as electrical plasma discharge proceeded the solution conductivity rised from  $3.0$  to  $3.87 \text{ mS cm}^{-1}$  after 24 min in Fig. S3.



Energy input is a determinant factor for active species generation and plasma treatment performance. As shown in Fig. S4, fluorescence intensity of 7-hydroxycoumarin produced from coumarin reacting with  $\cdot\text{OH}$  increased as a function of treatment time and energy input. This indicates larger amount of  $\cdot\text{OH}$  were produced at higher energy input. As a consequence, As(III) oxidation efficiency was enhanced by increasing the applied energy. For

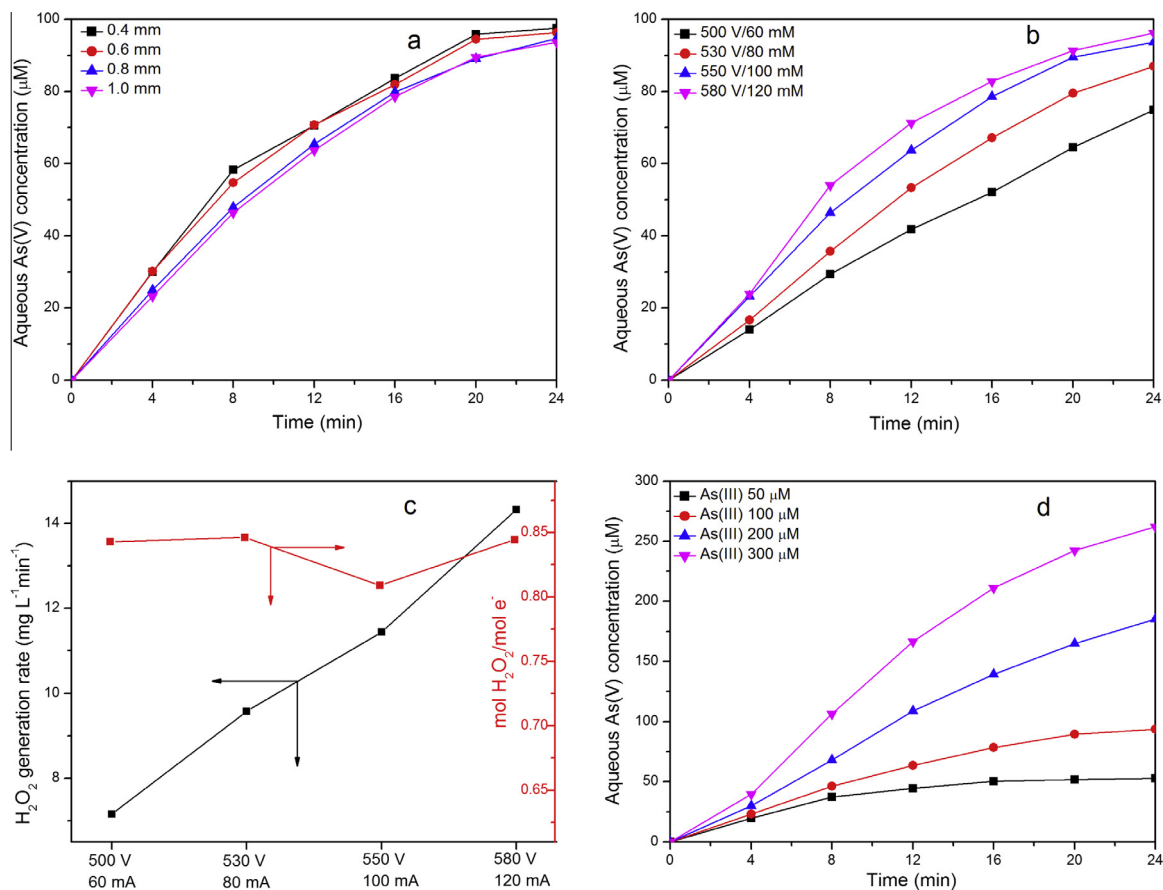


**Fig. 1.** Effect of different anode diameter on As(III) oxidation (a) and effect of input energy on As(V) formation (b) and H<sub>2</sub>O<sub>2</sub> generation (c), and effect of initial As(III) concentration on As(III) oxidation (d). (Typical condition: voltage, 550 V; current, 100 mA; pH, 4.0; As(III), 100 μM.)

example, when the applied voltage was 500 V, 530 V, 550 V and 580 V, the As(III) oxidation efficiency was 75%, 87%, 94% and 96%, respectively after 24 min (Fig. 1(b)).

In plasma generating process, the formed  $\cdot\text{OH}$  owns very short lifetime ( $3.7 \times 10^{-9}$  s) and is found abundant in the plasma zone (Jiang et al., 2014b). Thus, a competing reaction for  $\cdot\text{OH}$  was  $\cdot\text{OH}$  recombination with the generation of H<sub>2</sub>O<sub>2</sub>. As presented in Fig. 1(c), H<sub>2</sub>O<sub>2</sub> formation rate increased from  $7.2 \text{ mg L}^{-1} \text{ min}^{-1}$  to  $14.3 \text{ mg L}^{-1} \text{ min}^{-1}$  in As(III)-free Na<sub>2</sub>SO<sub>4</sub> solution with increasing voltage from 500 V to 580 V. Because of both the energy transfer (non-Faraday process) and charge transfer, the yields of H<sub>2</sub>O<sub>2</sub> in various energy input condition averagely corresponded to  $0.84 \text{ mol H}_2\text{O}_2 \text{ mol}^{-1} \text{ electron}$  higher than that expected from Faraday's law ( $0.5 \text{ mol H}_2\text{O}_2 \text{ mol}^{-1} \text{ electron}$ :  $\text{OH}^- - \text{e}^- \rightarrow 0.5\text{H}_2\text{O}_2$ ). In spite of abundant H<sub>2</sub>O<sub>2</sub> generation in CGDP and thermodynamically feasible for H<sub>2</sub>O<sub>2</sub> oxidizing As(III) (Eq. (3)), the direct oxidation rate for H<sub>2</sub>O<sub>2</sub> oxidizing As(III) was negligible ( $k_4 = 5.5 \times 10^{-3} \text{ M}^{-1} \text{ s}^{-1}$ ) at this pH in Eq. (4) (Pettine et al., 1999). Besides, we can observe no significant H<sub>2</sub>O<sub>2</sub> reduction for As(III)-containing solution in comparison with that in blank test in Fig. S5. Thus, the possibility that glow-generating H<sub>2</sub>O<sub>2</sub> acting as an oxidant of As(OH)<sub>3</sub> at pH 4.0 can be ruled out.

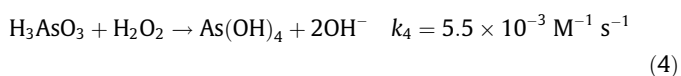
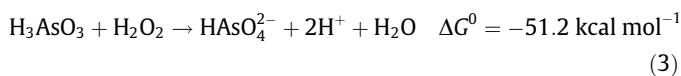


Fig. 1(d) shows higher initial concentration resulted in lower As(V) formation efficiency, but higher amount of As(III) oxidation. When the initial concentration was 50, 100, 200 or 300 μM, the As(III) oxidation efficiency was approximately 100%, 94%, 93% and 87%, respectively after 24 min CGDP treatment with corresponding the As(V) production amount of 0.56, 1.06, 2.09 and 2.94 mg, respectively.

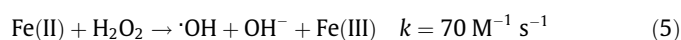
### 3.2. Oxidation and immobilization of arsenic mediated by Fenton reaction

It has been well illustrated that CGDP can produce a large number of H<sub>2</sub>O<sub>2</sub>, which contributed little for As(III) oxidation but provided a much more desirable condition for Fenton reactions (Jiang et al., 2014b). Besides, coagulation method utilizing iron ion as a flocculating agent is one of the most promising processes for arsenic immobilization from high arsenic-contaminated water because of the low cost and high efficiency (Song et al., 2006). Thus, it was rationally expected to add iron species in CGDP for simultaneous oxidation of As(III) and immobilization of arsenic species.

With the presence of 500 μM Fe(II) in As(III) solution, light brown turbidness in solution rapidly occurred upon exposure to CGDP. In this process, the concentration of aqueous As(V) increased to approximately 25 μM within 1.0 min but decreased afterward to approximately 0 μM; aqueous arsenic and iron continuously decreased in the whole treatment process with final immobilization efficiency of approximately 98% and 71%, respectively after 10 min; while in solid phase, the fraction of solid arsenic to total arsenic increased to 93%, in which nearly all of

the arsenic was present as As(V) in Table S1. In this process, the formed ionic As(V) rapidly coprecipitated with Fe(III) ions as ferric arsenate or was adsorbed on the ferric oxyhydroxides, which was produced via the hydrolysis reactions of aqueous Fe(III) ions (Tokoro et al., 2009). As for As(III) species, a negligible amount was detected owing to its high mobility in aqueous solution. The product of arsenic-bearing precipitation was poorly crystalline, which makes it difficult to characterize their arsenate phases using XRD as depicted in Fig. S6 (Langmuir et al., 2006; Stefánsson, 2007; Paktunc and Bruggeman, 2010; Zhao et al., 2010).

For comparison, As(III) oxidation in classical Fenton system at pH 4.0 were also carried out in this study. Fig. 2 demonstrates that the immobilization efficiencies of arsenic and iron species were less than those in CGDP system despite almost complete oxidation of As(III) when 120 mg L<sup>-1</sup> H<sub>2</sub>O<sub>2</sub> (the H<sub>2</sub>O<sub>2</sub> concentration produced in CGDP system at 10 min) was added at As(III)/Fe(II)-coexisting solution.



It was well known that Fe(II) reacts rapidly with H<sub>2</sub>O<sub>2</sub> to form Fe(III) accompanied by additional  $\cdot\text{OH}$  formation through reaction (5). Consequently, much more  $\cdot\text{OH}$  was produced in CGDP-Fe(II) system than that of CGDP system or Fenton system in Fig. 2(c). Furthermore, Hug and Leupin (Hug and Leupin, 2003) reported that Fe(IV) species can be produced due to faster reaction of Fe(II)- $\cdot\text{OH}$  in Fenton system, which can be a strong oxidant for the oxidations of As(III) and Fe(II). Thus, in CGDP-Fe(II) system, these two reasons may be collectively responsible for the fast As(V) formation and the consumption of Fe(II).

As regards many other advanced oxidation technologies for As(III) oxidation in Table S2, although appreciable As(III) oxidation efficiency can be obtained using these technologies, energy efficiencies were not only less than CGDP-Fenton system, but also failed to simultaneously immobilize arsenic from waters. Generally, CGDP-Fenton was a more efficient strategy for simultaneous oxidation and immobilization of arsenic. Furthermore, this process permitted to minimize the consumption of H<sub>2</sub>O<sub>2</sub> in-situ electro-generated in CGDP for As(III) oxidation and immobilization (SI Fig. S6), which therefore provides a potential of reutilization of this treated solution for other environmental remediation.

### 3.3. Effect of solution pH

In this study, we compared the As(V) formation efficiencies at pH range of 2.5–6.0 and found that varying solution pH in the range of 4.0–6.0 did not evidently influence As(III) oxidation efficiency in Fig. S7. According to Eq. (2), transforming As(III) to As(V) was accompanied with proton production and this is in accord with the reduce of pH in Fig. S3. Thus, high concentration of proton in extremely acidic solution greatly retarded As(III) oxidation. For example, As(V) formation reduced significantly from 93% to 72% at pH from 3.0 to 2.5 after 24 min treatment.

In the cases of adding Fe(II), solution pH is the critical factor for Fenton reaction, accumulation of ferric oxyhydroxides and formation of amorphous ferric arsenate (Stefánsson, 2007; Paktunc and Bruggeman, 2010). As shown in Fig. S8, the As(V) formation efficiency can rapidly reach approximately 100% within 1 min, which was independent of initial solution pH (2.5–6.0). These unanticipated results at slightly acidic solution may be not attributed to the reaction schemes that additional  $\cdot\text{OH}$  can form via chemical Fenton reaction but a different oxidant, namely Fe(IV) species, was produced at relatively high pH (Hug and Leupin, 2003). Conversely, the immobilization rates of arsenic and iron species in solution were significantly affected by solution pH (see in Fig. 3). For example, as pH was  $\leq 4.0$ , arsenic immobilization efficiency

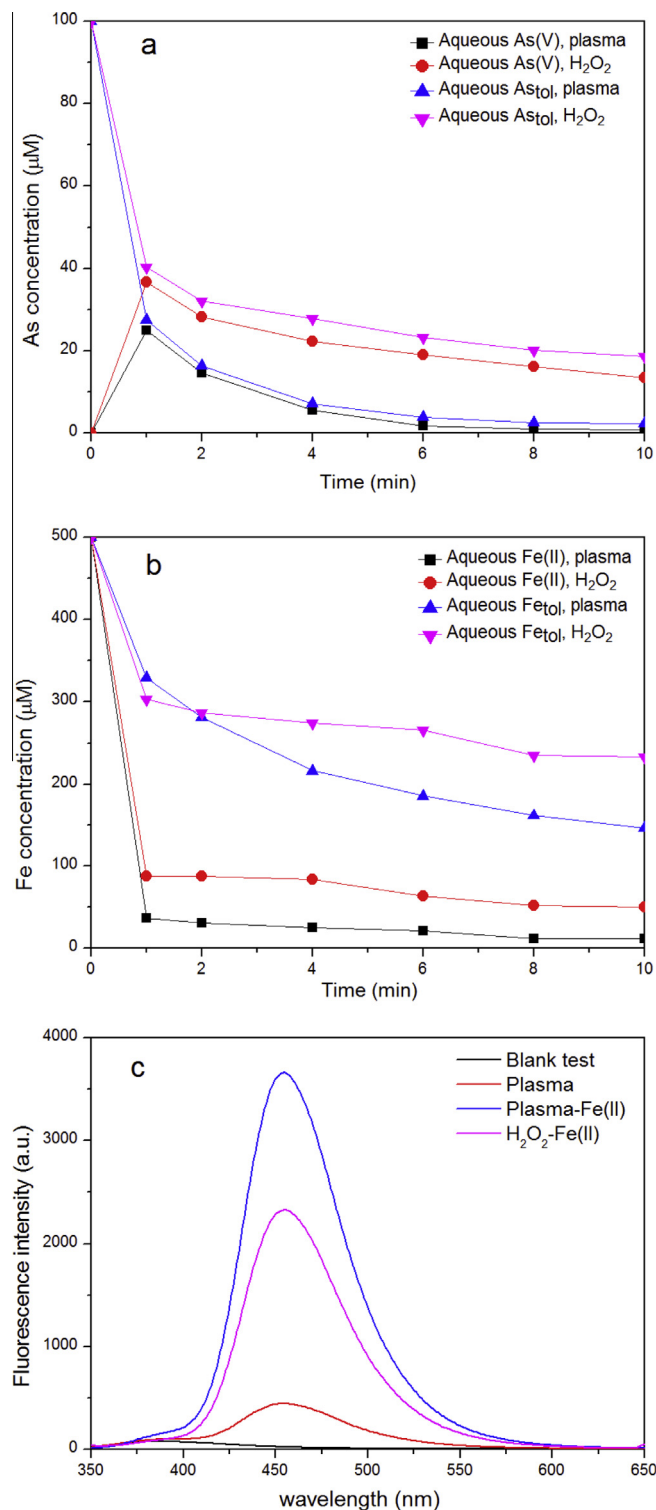


**Fig. 2.** Estimation of arsenic concentration and immobilization (a), iron concentration and precipitation (b) and the fluorescence intensity of 7-hydroxycoumarin produced within 4.0 min (c) in CGDE/Fenton system and classical Fenton system. (Typical condition: voltage, 550 V; current, 100 mA; pH, 4.0; As(III), 100  $\mu\text{M}$ ; Fe(II), 500  $\mu\text{M}$ .)

was evidently inhibited because of the high solubility of amorphous ferric arsenate at relatively strong acidic solution (Paktunc and Bruggeman, 2010). However, it took less than 10 min for the dissolved arsenic concentrations to drop below 3  $\mu\text{M}$  at pH 4.0–6.0, which satisfied the standard allowances of 500  $\mu\text{g L}^{-1}$  arsenic in industrial effluents (Chen et al., 2008).

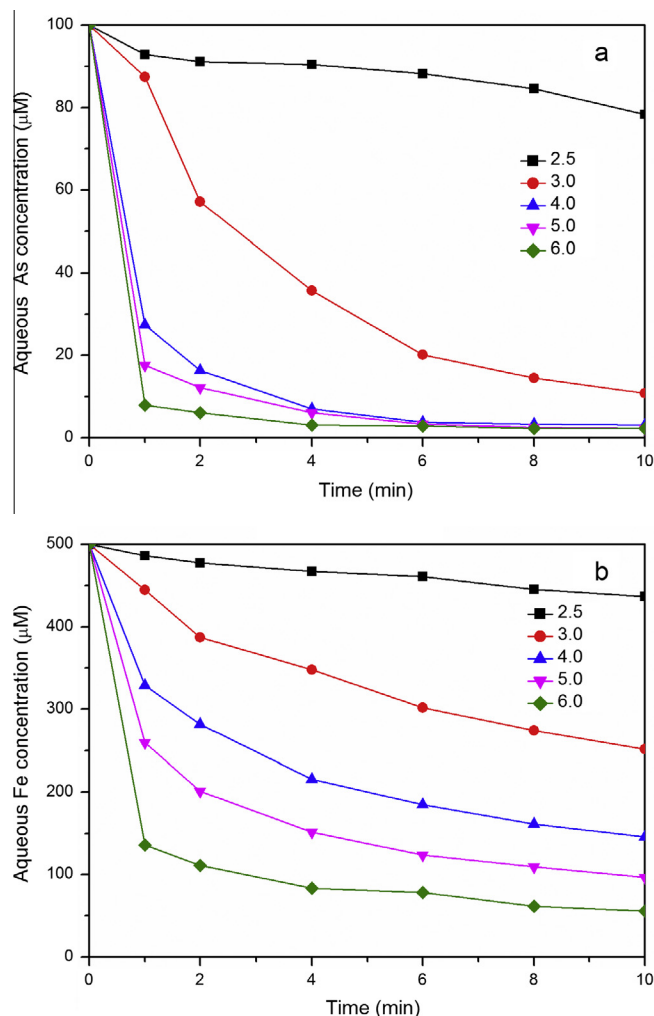


**Fig. 3.** Effect of solution pH on the immobilizations of arsenic and iron after 10 min CGDE treatment. (Typical condition: voltage, 550 V; current, 100 mA; As(III), 100 μM; Fe(II), 500 μM.)

#### 3.4. Effect of Fe(II) concentration

Since the Fenton reaction and the immobilization of arsenic are both closely related to the concentration of iron, a large range of Fe(II) addition from 100 to 1000 μM was studied in this section. As presented in Fig. S9, relatively high formation efficiency of As(V) can be obtained at Fe(II) concentration range of 250–1000 μM. It was expected that higher Fe(II) addition in As(III)-CGDP system could induce higher arsenic immobilization efficiency. However, after 10 min treatment, the optimal As immobilization efficiency was achieved at initial Fe(II) concentration of 500 μM whereas relatively slow arsenic immobilization rates for 1000 μM Fe(II) in Fig. 4. These results can be explained by the fact that during glow plasma generating process, the acidity of treated solution was enhanced through the hydrolysis reactions of free Fe(III) ions and this increasing trend was significantly greater at high concentration of Fe(II) addition as shown in Fig. 4, which therefore was prejudicial to the precipitations of iron and arsenic species.

With the increase in the initial Fe(II) concentration in As(III)-CGDP system, the color of precipitation changed from white grey at 100 μM Fe(II) to brown at 1000 μM Fe(II) (SI Fig. S10). Based on the mineral compositions of precipitations, it was calculated that the ratio of solid As/solid Fe was high, up to 0.74 for initial

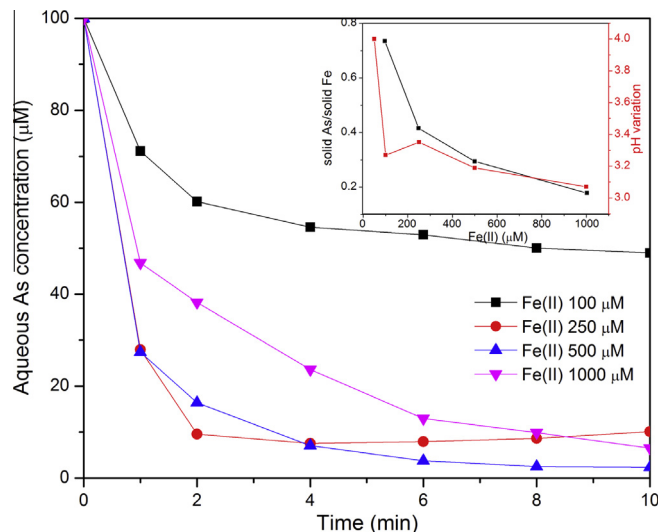


**Fig. 4.** Effect of Fe(II) concentration on arsenic immobilization after 10 min CGDE. Inset: effect of Fe(II) concentration on the ratio of solid As/solid Fe and pH variation. (Typical condition: voltage, 550 V; current, 100 mA; As(III), 100 μM; pH, 4.0.)

Fe(II) concentration of 100 μM and reduced significantly by raising Fe(II) addition. These results suggest that aqueous Fe(III) ions with relatively low concentration have an affinity towards reaction with As(V) rather than the formation of ferric hydroxide.

#### 3.5. Effect of organic and inorganic agents

As CGDP is applied for wastewater remediation, the presences of many organics in aqueous solution may exert various influence on treatment efficiency. Ethanol (EtOH) is a typical radical scavenger and has high reaction rate constant ( $1.9 \times 10^9 \text{ M}^{-1} \text{ s}^{-1}$ ) with  $\cdot\text{OH}$  (Liu, 2009; Jiang et al., 2014a). Fig. 5 shows that addition of EtOH retarded the arsenic immobilization efficiency by 14% after 10 min treatment. This can be ascribed to the facts that EtOH competed for  $\cdot\text{OH}$  with As(III) and Fe(II) leading to less As(V) formation in Fig. S11 and slower Fe(II) oxidation rate in Fig. 5(c).

Since Ox can effectively form complex with iron ions, which therefore stabilizes Fe(III) ions at a larger pH range and the reaction of the complex  $\text{FeC}_2\text{O}_4^0$  with  $\text{H}_2\text{O}_2$  ( $k_{\text{FeC}_2\text{O}_4+\text{H}_2\text{O}_2} = 3.1 \times 10^4 \text{ M}^{-1} \text{ s}^{-1}$ ) is three orders of magnitude faster than the reaction of Fe(II) and  $\text{H}_2\text{O}_2$  ( $k_{\text{Fe(II)}+\text{H}_2\text{O}_2} = 70 \text{ M}^{-1} \text{ s}^{-1}$ ) (Sedlak and Hoigné, 1993; Wang et al., 2013). Thus, in this content, the presence of Ox led to preferable As(III) oxidation efficiency (Fig. S11). However, the formed Fe(III)-oxalato complex can stabilize iron species in solution and hence greatly interrupted Fe precipitation reaction as well as the production of ferric arsenate in Fig. 5(b and d).

When phenol is present in CGDP-Fenton system, similar with the case of EtOH, its fast reaction rate with  $\cdot\text{OH}$  ( $k_{\text{phenol}+\cdot\text{OH}} = 1.2 \times 10^{10} \text{ M}^{-1} \text{ s}^{-1}$ ) greatly inhibited the oxidations of As(III) and Fe(II) (Fig. 5). For another, the hydroxycyclohexadienyl-like radicals produced from the attack of  $\cdot\text{OH}$  to phenol possessed reducing nature and can rapidly reduce Fe(III) ions to Fe(II) ions because they are prone to aromatise (Wang and Jiang, 2009). Consequently, the inhibitive oxidations of Fe(II) ions (Fig. 5(c)) and As(III) species (Fig. S11) together blocked the immobilizations of arsenic and iron from aqueous solution as shown in Fig. 5(b and d).

As depicted in Fig. S11 and Fig. 5, despite forming complexes with Fe(III), the presence of fluorion exhibited a lesser effect on the oxidation rates of As(III) and arsenic immobilization. In this case, arsenic immobilization efficiency was comparable to that in the case free of fluorion but with less Fe(III) precipitation.

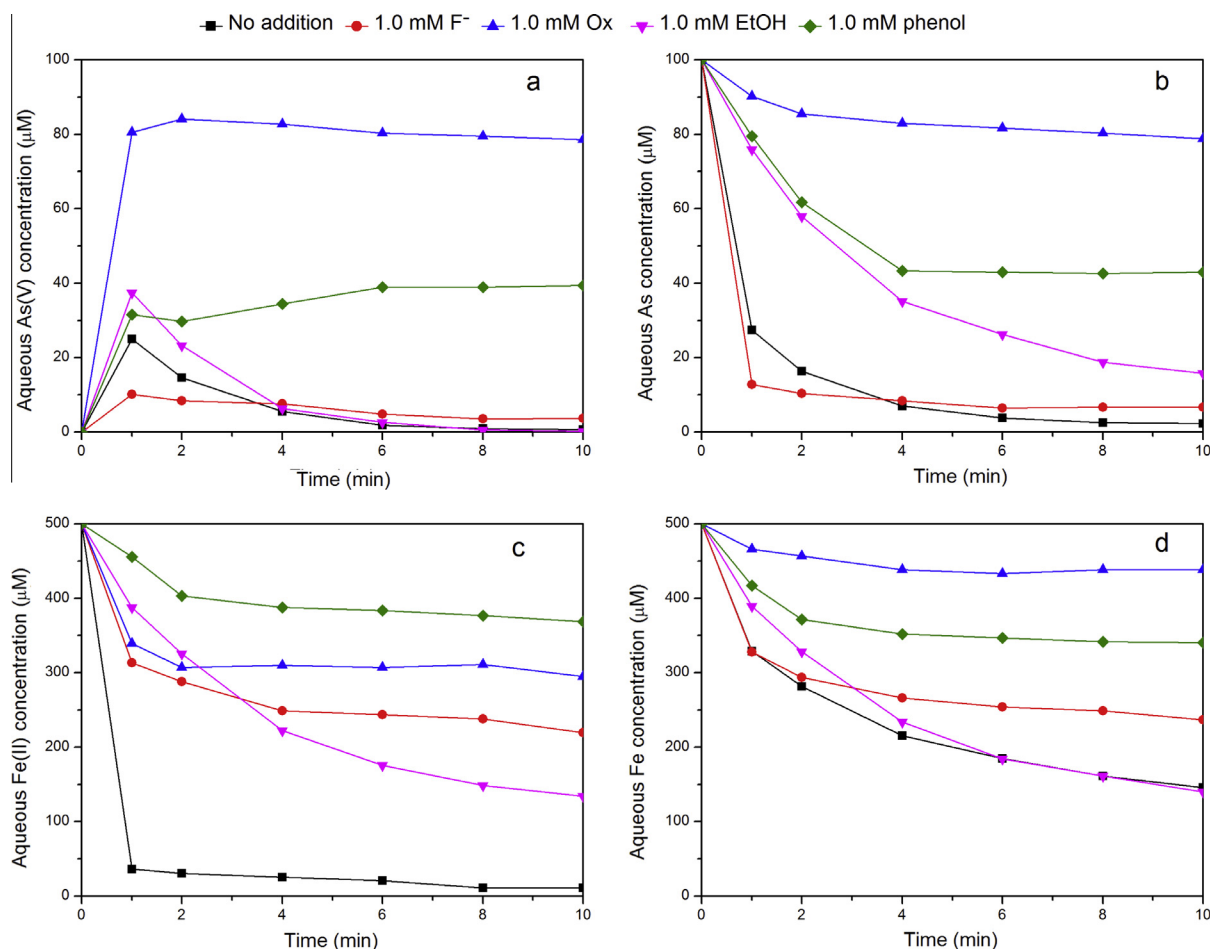


**Fig. 5.** Effect of organic and inorganic additions on As(V) formation, arsenic immobilization, Fe(II) oxidation and iron immobilization. (Typical condition: voltage, 550 V; current, 100 mA; As(III), 100 μM; pH, 4.0; Fe(II), 500 μM.)

In conclusion, the presence of organics that can stabilize iron ions, or scavenging  $\cdot\text{OH}$  would inhibit the oxidation of As(III) and arsenic immobilization in CGDP-Fenton system. As for inorganic Fe(III) ligand, namely fluorion, although it can effectively restrain the precipitation of iron ions from water, lesser influence was observed for arsenic immobilization. Thus, the effects of these additions on arsenic immobilization efficiency depended on their complexing capacities with iron ions or capabilities of scavenging  $\cdot\text{OH}$ .

#### 4. Conclusions

In this study, simultaneous oxidation and immobilization of arsenic species can be achieved using CGDP-Fenton system. Solution pH and initial Fe(II) concentration were both significant factors for arsenic immobilization. In this process, the formed ionic As(V) rapidly coprecipitated with Fe(III) ions or was adsorbed on the ferric oxyhydroxides with the formation of amorphous ferric arsenate-bearing ferric oxyhydroxides. Above, CGDP can create a well-controlled artificial environment favoring oxidative immobilization of aqueous arsenic, which can serve as a remediation strategy for arsenic-containing wastewater remediation.

#### Acknowledgments

This work is financially supported by National Natural Science Foundation of China (Nos. 21376268, 21176260, 51372277, 21302224), the National Basic Research Development Program of

China (973 Program) (No. 2011CB605703), the Taishan Scholar Foundation (No. ts20130929) and Fundamental Research Funds for the Central Universities (No. 14CX06117A).

#### Appendix A. Supplementary material

Supplementary data associated with this article can be found, in the online version, at <http://dx.doi.org/10.1016/j.chemosphere.2014.12.056>.

#### References

- Bissen, M., Frimmel, F.H., 2003. Arsenic—a review. Part II: oxidation of arsenic and its removal in water treatment. *Acta Hydroch. Hydrob.* 31, 97–107.
- Chen, C.Y., Chang, T.H., Kuo, J.T., Chen, Y.F., Chung, Y.C., 2008. Characteristics of molybdate-impregnated chitosan beads (MICB) in terms of arsenic removal from water and the application of a MICB-packed column to remove arsenic from wastewater. *Bioresour. Technol.* 99, 7487–7494.
- Chen, J., Pan, X., Chen, J., 2013. Regeneration of activated carbon saturated with odors by non-thermal plasma. *Chemosphere* 92, 725–730.
- Choi, W., Yeo, J., Ryu, J., Tachikawa, T., Majima, T., 2010. Photocatalytic oxidation mechanism of As(III) on TiO<sub>2</sub>: unique role of As(III) as a charge recombinant species. *Environ. Sci. Technol.* 44, 9099–9104.
- Dhar, R.K., Zheng, Y., Rubenstone, J., van Geen, A., 2004. A rapid colorimetric method for measuring arsenic concentrations in groundwater. *Anal. Chim. Acta* 526, 203–209.
- Eisenberg, G., 1943. Colorimetric determination of hydrogen peroxide. *Ind. Eng. Chem. Anal. Ed.* 15, 327–328.
- Gräfe, M., Nachttegaal, M., Sparks, D.L., 2004. Formation of metal–arsenate precipitates at the goethite–water interface. *Environ. Sci. Technol.* 38, 6561–6570.
- Hug, S.J., Leupin, O., 2003. Iron-catalyzed oxidation of arsenic (III) by oxygen and by hydrogen peroxide: pH-dependent formation of oxidants in the Fenton reaction. *Environ. Sci. Technol.* 37, 2734–2742.

- Ishibashi, K.-I., Fujishima, A., Watanabe, T., Hashimoto, K., 2000. Detection of active oxidative species in  $\text{TiO}_2$  photocatalysis using the fluorescence technique. *Electrochem. Commun.* 2, 207–210.
- Jiang, B., Guo, J., Wang, Z., Zheng, X., Zheng, J., Wu, W., Wu, M., Xue, Q., 2014a. A green approach towards simultaneous remediations of Chromium (VI) and Arsenic (III) in aqueous solution. *Chem. Eng. J.* 262, 1144–1151.
- Jiang, B., Zheng, J., Qiu, S., Wu, M., Zhang, Q., Yan, Z., Xue, Q., 2014b. Review on electrical discharge plasma technology for wastewater remediation. *Chem. Eng. J.* 236, 348–368.
- Khuntia, S., Majumder, S.K., Ghosh, P., 2014. Oxidation of As(III) to As(V) using ozone microbubbles. *Chemosphere* 97, 120–124.
- Langmuir, D., Mahoney, J., Rowson, J., 2006. Solubility products of amorphous ferric arsenate and crystalline scorodite ( $\text{FeAsO}_4 \cdot 2\text{H}_2\text{O}$ ) and their application to arsenic behavior in buried mine tailings. *Geochim. Cosmochim. Acta* 70, 2942–2956.
- Lescano, M.R., Zalazar, C.S., Cassano, A.E., Brandi, R.J., 2011. Arsenic (iii) oxidation of water applying a combination of hydrogen peroxide and UVC radiation. *Photochem. Photobiol. Sci.* 10, 1797–1803.
- Liu, R., Guo, Y., Wang, Z., Liu, J., 2014. Iron species in layered clay: efficient electron shuttles for simultaneous conversion of dyes and Cr(VI). *Chemosphere* 95, 643–646.
- Liu, Y., 2009. Simultaneous oxidation of phenol and reduction of Cr(VI) induced by contact glow discharge electrolysis. *J. Hazard. Mater.* 168, 992–996.
- Mohan, D., Pittman Jr, C.U., 2007. Arsenic removal from water/wastewater using adsorbents—a critical review. *J. Hazard. Mater.* 142, 1–53.
- Neppolian, B., Doronila, A., Ashokkumar, M., 2010. Sonochemical oxidation of arsenic(III) to arsenic(V) using potassium peroxydisulfate as an oxidizing agent. *Water Res.* 44, 3687–3695.
- Paktunc, D., Bruggeman, K., 2010. Solubility of nanocrystalline scorodite and amorphous ferric arsenate: implications for stabilization of arsenic in mine wastes. *Appl. Geochem.* 25, 674–683.
- Pettine, M., Campanella, L., Millero, F.J., 1999. Arsenite oxidation by  $\text{H}_2\text{O}_2$  in aqueous solutions. *Geochim. Cosmochim. Acta* 63, 2727–2735.
- Sedlak, D.L., Hoigné, J., 1993. The role of copper and oxalate in the redox cycling of iron in atmospheric waters. *Atmos. Environ. Part A* 27, 2173–2185.
- Song, S., Lopez-Valdivieso, A., Hernandez-Campos, D., Peng, C., Monroy-Fernandez, M., Razo-Soto, I., 2006. Arsenic removal from high-arsenic water by enhanced coagulation with ferric ions and coarse calcite. *Water Res.* 40, 364–372.
- Stefánsson, A., 2007. Iron (III) hydrolysis and solubility at 25 °C. *Environ. Sci. Technol.* 41, 6117–6123.
- Tokoro, C., Yatsugi, Y., Koga, H., Owada, S., 2009. Sorption mechanisms of arsenate during coprecipitation with ferrihydrite in aqueous solution. *Environ. Sci. Technol.* 44, 638–643.
- Wang, L., Jiang, X., 2009. Unusual catalytic effects of iron salts on phenol degradation by glow discharge plasma in aqueous solution. *J. Hazard. Mater.* 161, 926–932.
- Wang, Z., Bush, R.T., Liu, J., 2013. Arsenic(III) and iron(II) co-oxidation by oxygen and hydrogen peroxide: divergent reactions in the presence of organic ligands. *Chemosphere* 93, 1936–1941.
- Wang, Z., Bush, R.T., Sullivan, L.A., Chen, C., Liu, J., 2014. Selective oxidation of arsenite by peroxydisulfate with high utilization efficiency of oxidant. *Environ. Sci. Technol.* 48, 3978–3985.
- Zhang, Y., Zheng, J., Qu, X., Chen, H., 2008. Design of a novel non-equilibrium plasma-based water treatment reactor. *Chemosphere* 70, 1518–1524.
- Zhao, X., Zhang, B., Liu, H., Qu, J., 2010. Removal of arsenite by simultaneous electro-oxidation and electro-coagulation process. *J. Hazard. Mater.* 184, 472–476.